Laboratori Nazionali di Frascati

LNF-62/72 (1962)

C. Infante, F. Pandarese: THE TUNNEL DIODE AS A THRESHOLD DEVICE: THEORY AND APPLICATION.

Estratto dal: Proceeding of the Conference on Nuclear Electronics, Belgrade, may 1961 (IAEA, Vienna, 1962), Vol. III, pag. 29.

THE TUNNEL DIODE AS A THRESHOLD DEVICE: THEORY AND APPLICATION

G. INFANTE AND F. PANDARESE
COMITATO NAZIONALE PER L'ENERGIA NUCLEARE
LABORATORI NAZIONALI DI FRASCATI
ITALY

Abstract — Résumé — Аннотация — Resumen

The tunnel diode as a threshold device: theory and application. Due to the interesting properties of the tunnel diode, the device is extensively studied concerning its circuit behaviour. An empirical formula, approximating the diode's V-I characteristics, has been obtained. This allows calculations of rise time, delay time, jitter, etc., to be carried out in certain instances; theoretical predictions based on this approximation are in good agreement with experimental results. Stability considerations and curve-plotting circuits are also studied. A high-speed discriminator-coincidence circuit using transistors and tunnel diodes is presented.

La diode tunnel employée comme discriminateur de seuil; théorie et application. Les propriétés intéressantes de la diode tunnel permettent d'étudier dans le détail son comportement dans un circuit. L'auteur a obtenu une formule empirique qui donne une approximation des caractéristiques V-I de la diode et permet de procéder dans certains cas au calcul du temps de montée, des instabilités de retard, etc.; les prédictions théoriques fondées sur cette approximation concordent avec les résultats expérimentaux. L'auteur étudie aussi les problèmes de stabilité et les circuits de tracé des courbes. Il présente un circuit à discriminateur rapide et à coïncidence utilisant des transistors et des diodes tunnel.

Применение туннельного диода в качестве порогового устройства; теория и ее применение. Ввиду особо интересных свойств туннельного диода, это устройство тщательно изучается с точки зрения поведения его контура. Была получена эмпирическая формула, дающая приближенное значение характеристик V-I диода. Это дает возможность подсчитывать время нарастания, разброс времени задержки и т.д., которые наблюдаются в некоторых случаях; теоретический прогноз, основанный на этом приближении, хорошо совпадает с экспериментальными результатами. Исследуются также соображения устойчивости и контуры построения кривых. Дается описание высокоскоростного дискриминатора, имеющего схему совпадений и работающего на транзисторах и туннельных диодах.

El diodo de túnel como dispositivo de umbral: teoría y aplicación. Debido a las interesantes propiedades que presenta, el diodo de túnel se estudia extensamente en la memoria desde el punto de vista de su comportamiento en circuitos. Se ha obtenido una fórmula empírica que corresponde aproximadamente a la característica V-I del diodo. Esto permite calcular, en ciertos casos, el tiempo de elevación, el tiempo de retardo, la inestabilidad, etc.; los valores calculados teóricamente mediante esta fórmula aproximada concuerdan satisfactoriamente con los resultados obtenidos experimentalmente. El autor examina también los factores de estabilidad y los circuitos para el trazado de las características. En la memoria se presenta un discriminador de alta velocidad y circuito de coincidencia, en el que se emplean transistores y diodos de túnel.

I. Introduction

Tunnel diodes or Esaki diodes [1] are finding increasingly large applications as high-frequency devices [2—5]: this is due to the intrinsically good high-frequency properties of the device coupled with other desirable properties such as small size, low power consumption, stability of characteristics with respect to temperature, commercial availability and, last but not least, low cost with respect to transistors having gain-band-width

products of the same order of magnitude. The device is thus extremely promising and is being extensively studied regarding its application in computer technology [6].

The above reasons have prompted the authors to study the device with the intention of applying it in the field of high-speed electronics in the nuclear field.

II. The V-I characteristic and its approximation

One of the most striking features of the tunnel diode (TD) is the peculiar shape of its V—I characteristic (Fig. 1).

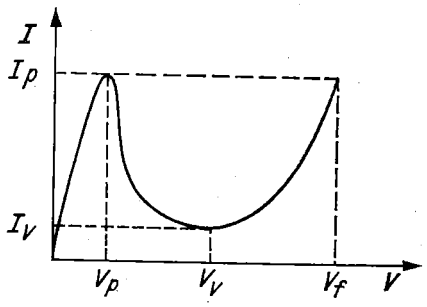

Fig. 1
Tunnel diode characteristic

Small signal theory approximates the characteristic with a constant (differential) resistance whose magnitude is positive or negative, according to the bias point chosen. This approach fails, of course, when dealing with large signals (i.e. switching circuitry). Although piece-meal linear approximation has been attempted with success [7—8], a higher order of approximation has been studied with the purpose of excluding the discontinuities of the differential conductance function.

Under the assumptions

(a) That the approximating function be continuous with its first order derivatives over the range of interest (0 to V_f), and

(b) That the function should not be higher than 2 (i.e. two parabolas joined at some intermediate point v_x) the following approximation has been derived:

$$i = I_p \left[1 - \left(\frac{v}{v_p} - 1\right)^2\right] \qquad \text{for} \qquad 0 \leqslant v \leqslant v_x \tag{1}$$

$$i = K(v - v_v)^2 + I_v \qquad \text{for} \qquad v_x \leqslant v \leqslant v_f \tag{2}$$

where $K = \dfrac{AI_p - I_v}{(v_x - v_v)^2}$, $v_x = v_p \dfrac{\left(\frac{v_v}{v_p} - \frac{I_v}{I_p}\right)}{\left(\frac{v_v}{v_p} - 1\right)}$, $A = 1 - \dfrac{\left(1 - \frac{I_v}{I_p}\right)^2}{\left(1 - \frac{v_v}{v_p}\right)^2}$.

No justification of the formula on the basis of solid-state theory will be attempted; the closeness of the fit is shown by the accompanying Figures (2 and 3) in which measured points of commercial diodes are compared with theoretical predictions based on equa-

tions (1) and (2). The fit is quite good in the low-voltage region, fairly good in the negative resistance region and very poor in the high-voltage region where the exponential increase of current, due to minority carrier injection, is much faster than the parabolic increase provided by (2).

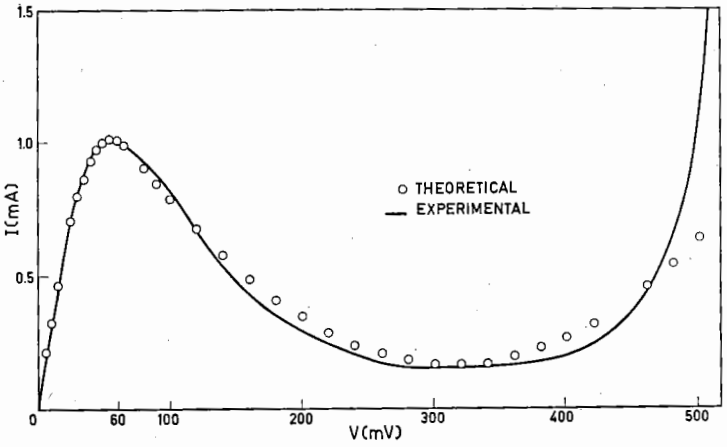

Fig. 2

Theoretical and measured characteristics of commercial tunnel-diode types

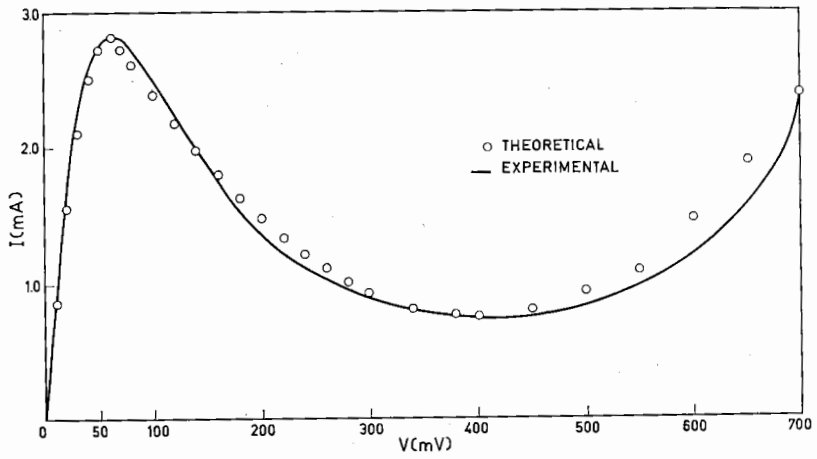

Fig. 3

Theoretical and measured characteristics of commercial tunnel-diode types

It may be interesting to note that the absolute value of the differential negative resistance has its minimum in v_x, its value being

$$\left| r_{neg} \right|_{min} = \left[\frac{1}{\frac{di}{dv}} \right]_{v = v_x} = \frac{v_p^2}{2 I_p} \frac{1}{v_x - v_p}. \tag{3}$$

Both equations (1) and (2) may be written as

$$i = f(v) = K_1 (v - v_0)^2 + K_2 \tag{4}$$

with appropriate parameter substitution.

III. Response to a current step waveform

Neglecting lead inductance, the TD can be thought of as a non-linear element defined by its static V—I characteristic shunted by a capacitance C (9), (Fig. 4.)

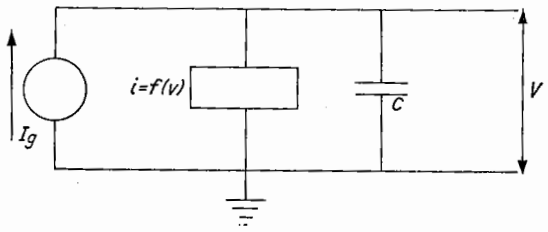

Fig. 4
Equivalent circuit of the tunnel diode. Response to a current step

From the circuit equation, the time t necessary for the voltage V to go from 0 to a value v is given by

$$t = c \int_0^v \frac{dv}{I_g - f(v)} + K$$

where K is an integration constant that depends on the initial conditions. Substituting (1) and (2) one finds that switching time (to go from 0 to v_f) is given by

$$\tau = \tau_{S1} + \tau_{S2} \tag{5}$$

where

$$\tau_{S1} = \frac{-v_p^2 C}{I_p C_1} \operatorname{tg}^{-1}\left(-\frac{v_p}{C_1}\right) + \frac{v_p^2 C}{I_p C_1} \operatorname{tg}^{-1}\left(\frac{v_x - v_p}{C_1}\right), \quad \text{with} \quad C_1 = v_p \sqrt{\frac{I_g}{I_p} - 1},$$

is the time to go from 0 to v_x and

$$\tau_{S2} = \frac{C (v_x - v_v)}{\sqrt{(I_g - I_v)(A I_p - I_v)}} \left[\operatorname{tgh}^{-1}\left(\frac{v_f - v_v}{C_2}\right) - \operatorname{tgh}^{-1}\left(\frac{v_x - v_v}{C_2}\right) \right] \tag{5'}$$

is the time to go from v_x to v_f, with

$$C_2 = \sqrt{\frac{I_g - I_v}{A I_p - I_v}} (v_x - v_v).$$

Examination of equations (5) and (5′) shows that the predominant term is τ_{S_1}, which depends strongly on I_g the input current-step amplitude. Equation (5′) is in good agreement with experimental results, a plot of τ_{S_1} *vs.* I_g yielding the familiar regenerative circuit delay curve [10].

IV. Response to a voltage step

For the circuit, shown in Fig. 5

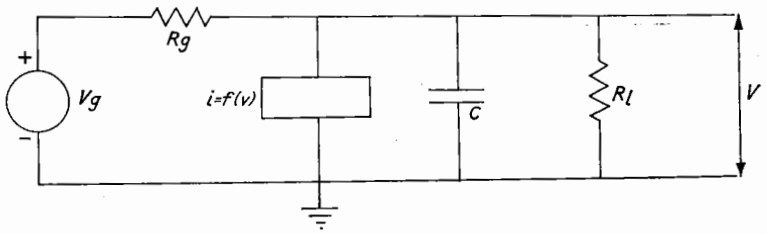

Fig. 5
Equivalent circuit of the tunnel diode. Response to a voltage step

one finds the equation

$$t = C \int_0^v \frac{\mathrm{d}v}{\frac{v_g}{R_g} - f(v) - \frac{v}{R_p}} \tag{6}$$

where

$$R_p = \frac{R_L R_g}{R_L + R_g}$$

hence, with the notations employed in the preceding paragraph,

$$\tau_{S1} = \frac{2C}{\sqrt{q}} \left[\mathrm{tg}^{-1} \frac{\frac{2I_p}{v_p^2}(v_2 - v_p) - \frac{1}{R_p}}{\sqrt{q}} - \mathrm{tg}^{-1} \frac{2\frac{I_p}{v_p} + \frac{1}{R_p}}{-\sqrt{q}} \right], \tag{7}$$

$$\tau_{S2} = \frac{2C}{\sqrt{-q}} \left[\mathrm{tgh}^{-1} \frac{-2\frac{AI_p - I_v}{(v_x - v_v)^2}(v_f - v_v) - \frac{1}{R_p}}{\sqrt{-q}} - \mathrm{tgh}^{-1} \frac{-2\frac{AI_p - I_v}{(v_x - v_v)} - \frac{1}{R_p}}{\sqrt{-q}} \right],$$

where

$$q = \frac{4I_p}{v_p^2}\left(\frac{v_g}{R_g} - I_p - \frac{v_p}{R_p}\right) - \frac{1}{R_p^2}.$$

As will be seen in paragraph 7 experimental results are in good agreement with these predictions.

The addition of series inductance L, leads to a differential equation of the following type:

$$\frac{d^2v}{dt^2} + \left[\frac{1}{C}\frac{df}{dv} + \frac{R_g}{L}\right]\frac{dv}{dt} + \frac{R_g f(v) + v - v_g}{LC} = 0 \tag{8}$$

which is not soluble in an elementary fashion.

V. Response to a voltage ramp

For the circuit of Fig. 6

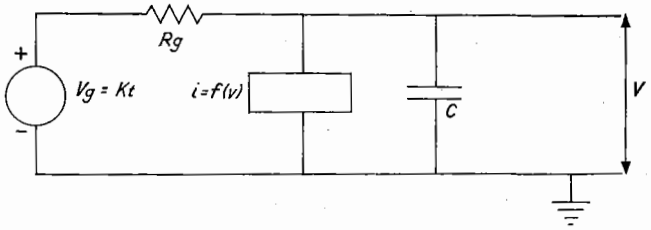

Fig. 6
Equivalent circuit of the tunnel diode. Response to a voltage ramp

the equation is

$$C\frac{dv}{dt} + f(v) = \frac{Kt - v}{R_g} \tag{9}$$

whose solution is

$$v = v_0 + \frac{1}{2R_g K_1} - \frac{b''^{\frac{1}{3}}}{2az} - \frac{b''^{\frac{1}{3}}}{a}\sqrt[3]{\zeta}\,\frac{C_1 I'_{\frac{1}{3}} + I'_{-\frac{1}{3}}}{C_1 I_{\frac{1}{3}} + I_{-\frac{1}{3}}}$$

where

$$C_1 = \frac{I'_{-\frac{1}{3}}\left(\frac{2}{3}z_0^3\right) - \frac{M}{\sqrt{z_0}} I'_{-\frac{1}{3}}\left(\frac{2}{3}z_0^3\right)}{\frac{M}{\sqrt{z_0}} I_{\frac{1}{3}}\left(\frac{2}{3}z_0^3\right) - I_{\frac{1}{3}}\left(\frac{2}{3}z_0^3\right)}$$

is the integration constant, determined by setting $v = 0$ for $t = 0$. The slope of the output voltage waveform, i.e.

$$\frac{dv}{dt} = -\frac{1}{a}\left[\frac{b''^2}{(a'' + b''t)^2} + \frac{a''}{(a'' + b''t)}\left[\frac{C_1 I'_{\frac{1}{3}} + I'_{-\frac{1}{3}}}{C_1 I_{\frac{1}{3}} + I_{-\frac{1}{3}}}\right] + \right.$$
$$\left. + \tfrac{1}{2}(a'' + b''t)\frac{d}{d\chi}\left(\frac{C_1 I'_{\frac{1}{3}} + I'_{-\frac{1}{3}}}{C_1 I_{\frac{1}{3}} + I_{-\frac{1}{3}}}\right)\right] \tag{10}$$

is only slightly dependent on K (the input voltage-slope) for values of v close to v_x because the two first terms largely cancel each other. This verifies a well-known experimental fact. In the above equations the following symbols have been used

$$b''^{\frac{1}{3}}\zeta = a'' + b''t; \qquad \zeta_0 = \frac{a''}{b''^{\frac{1}{3}}}$$

$$a'' = \frac{K_1}{C}\left(\frac{v_0}{R_g C} + \frac{K_2}{C}\right) - \frac{1}{4 R_g^2 C^2}$$

$$b'' = \frac{K_1}{C^2 R_g} \mathrm{K}\,; \qquad a = -\frac{K_1}{C}\,; \qquad I_j = I_j\left(\tfrac{2}{3} z^{\frac{3}{2}}\right)$$

$$-M = \frac{1}{2 z_0} + \frac{a'}{2 b''^{\frac{1}{3}}} + \frac{a v_0}{b''^{\frac{1}{3}}}$$

$$\chi = \tfrac{2}{3} |z_0|^{\frac{3}{2}}\,.$$

VI. General considerations

Due to the negative resistance region of the TD's characteristic, it is quite possible for the device to oscillate when biased in this region. This fact poses a certain number of practical difficulties in designing suitable curve tracers to display the V—I curve. It has been shown [11] that, for a negative resistance $-r$ to be stable when shunted by a positive resistance R, the following inequalities must hold

$$\frac{L}{r C} < R < r$$

where L and C are *total* series inductance and shunt capacitance respectively. Since

$$r = \left|\frac{\mathrm{d}V}{\mathrm{d}i}\right| = 1 \Big/ \left|\frac{\mathrm{d}i}{\mathrm{d}V}\right|$$

is a function of voltage, the above relation must be verified for all r, i.e. for the minimum value that r may take over this range, i.e.

$$\frac{L}{r_{\min} C} < R < r_{\min}$$

where $r_{\min}$ is given by equation (3).

Let us now consider the circuit shown in Fig. 7.

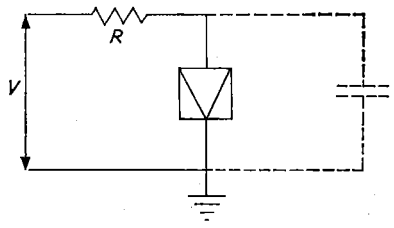

Fig. 7
Amplitude discriminator circuit

For each value of V a load in the conventional manner can be drawn, and it is easily seen that the circuit will jump from a low to a high-voltage state (provided R is large enough) when

$$V \gtrsim v_p + R I_p$$

so that this simple circuit will act as a trigger or amplitude-discriminator circuit. Input-output diagrams for a range of resistances are given in Fig. 8. It is a well-known fact that loop gain-bandwidth is the major factor influencing speed and threshold definition of

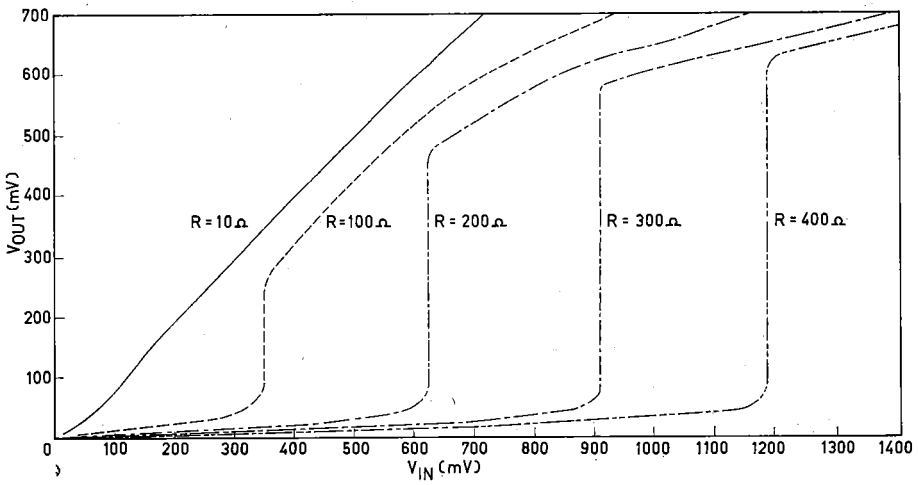

Fig. 8
Input-output voltage characteristics for the circuit of Fig. 7, with tunnel diode HT-16

trigger circuits [11—12]. Loop gain-bandwidth (GBW) products are easily calculated only assuming linearity: for non-linear circuits a comparison may be made by calculating the GBW at maximum gain. For the tunnel-diode circuit above one obtains, again neglecting circuit inductance,

$$\mathrm{GBW} \simeq \frac{g}{2\pi} \frac{1 + R_g}{C} \text{ Mc/s}$$

where $g = \dfrac{1}{\gamma_{\min}}$. For a 1-mA, 10-pF TD (tunnel diode) (13) one obtains,

$$\mathrm{GBW} \simeq 1.2 \times 10^9 \text{ Mc/s},$$

whereas for a 50-mA, 25-pF TD (14) one obtains

$$\mathrm{GBW} \simeq 24 \times 10^9 \text{ Mc/s}.$$

In contrast, for a vacuum-tube trigger circuit using wide-band pentodes (E 180F's) in a conventional arrangement, one finds

$$\mathrm{GBW} \simeq 0.35 \times 10^9 \text{ Mc/s}.$$

The above figures clearly indicate the advantage of using tunnel diodes for such circuits.

VII. Fast discriminator-coincidence circuit

The block diagram of the fast discriminator-coincidence circuit is given in Fig. 9. Input pulses greater than pre-set thresholds trigger the TD discriminators which in turn

trigger the coincidence proper, which is therefore fed by standard pulses. Use of discriminators preceding the coincidence allows a large reduction in chance coincidences due to the low-level background to be made. Circuit diagram is given in Fig. 10.

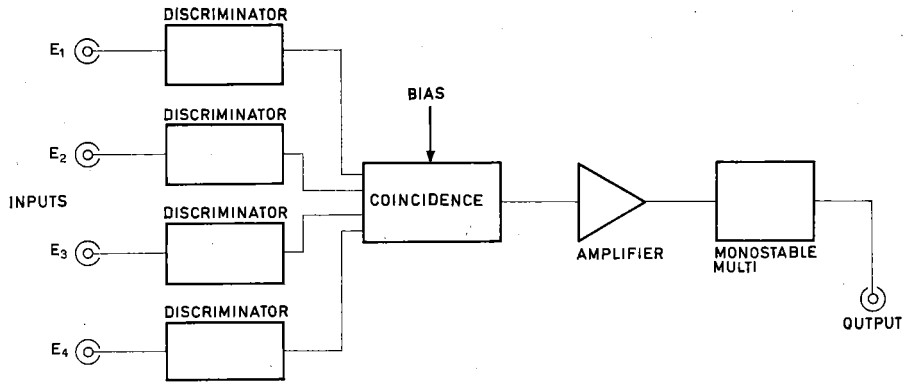

Fig. 9
Block diagram of fast coincidence circuit

Tunnel diode TD1 is current-biased by DC emitter-follower Q_1, diode D_1 being added to improve the discriminator's linearity in the high ranges. Negative input pulses above the threshold trigger TD_1 are emitter-followed by Q_2 and turn on Q_3. As Q_3 is normally off, this reduces pedestal and feed-through problems. Current drawn by transistor Q_4 is almost entirely determined by its emitter resistor and by the positive voltage supply. When Q_4 is turned off it therefore produces a standard pulse which is clipped by the subsequent shorting stub. Each discriminator therefore feeds a standard current pulse in TD_2; depending on the biasing conditions, the number of pulses necessary to trigger TD_2 may be 2,3 or 4. Selection is accomplished by rotating switch S_1, thereby changing the order of coincidence. Anti-coincidence is accomplished simply by inverting the pulse produced by a discriminator, i.e. reversing one of the windings of pulse transformer T_1. When TD_2 triggers, its (negative) output is amplified by a long-tailed pair, Q_5 and Q_6, thereby firing the monostable circuit composed of Q_7, Q_8 and Q_9 [16]. Q_{10} is added for impedance matching. Output is 5 V (positive or negative) into 125 Ω, 50-ns duration. As the input impedance of the circuit is not well-defined, it is imperative that connecting cables be correctly matched at the photomultiplier end.

The discriminator calibration curve is shown in Fig. 11, while the delay-time jitter (for long pulses) is shown in Fig. 12 and agrees well with theoretical predictions based on the foregoing theory. Delay-time jitter for short (20 ns) pulses is much less, about 5 ns for a pulse whose amplitude is 1% above threshold. The discriminator's dead time is about 50 ns and it will trigger up to about 20 Mc. Coincidence resolving time is quite good: the accompanying Fig. 13 shows a full-width at half-maximum of 4 ns. The curve was taken using cosmic rays detected by two 28 × 10 × 1 cm plastic scintillators viewed by RCA 6810A photomultipliers and is therefore almost entirely due to the photostatistics. Clipping stubs were 5 ns long.

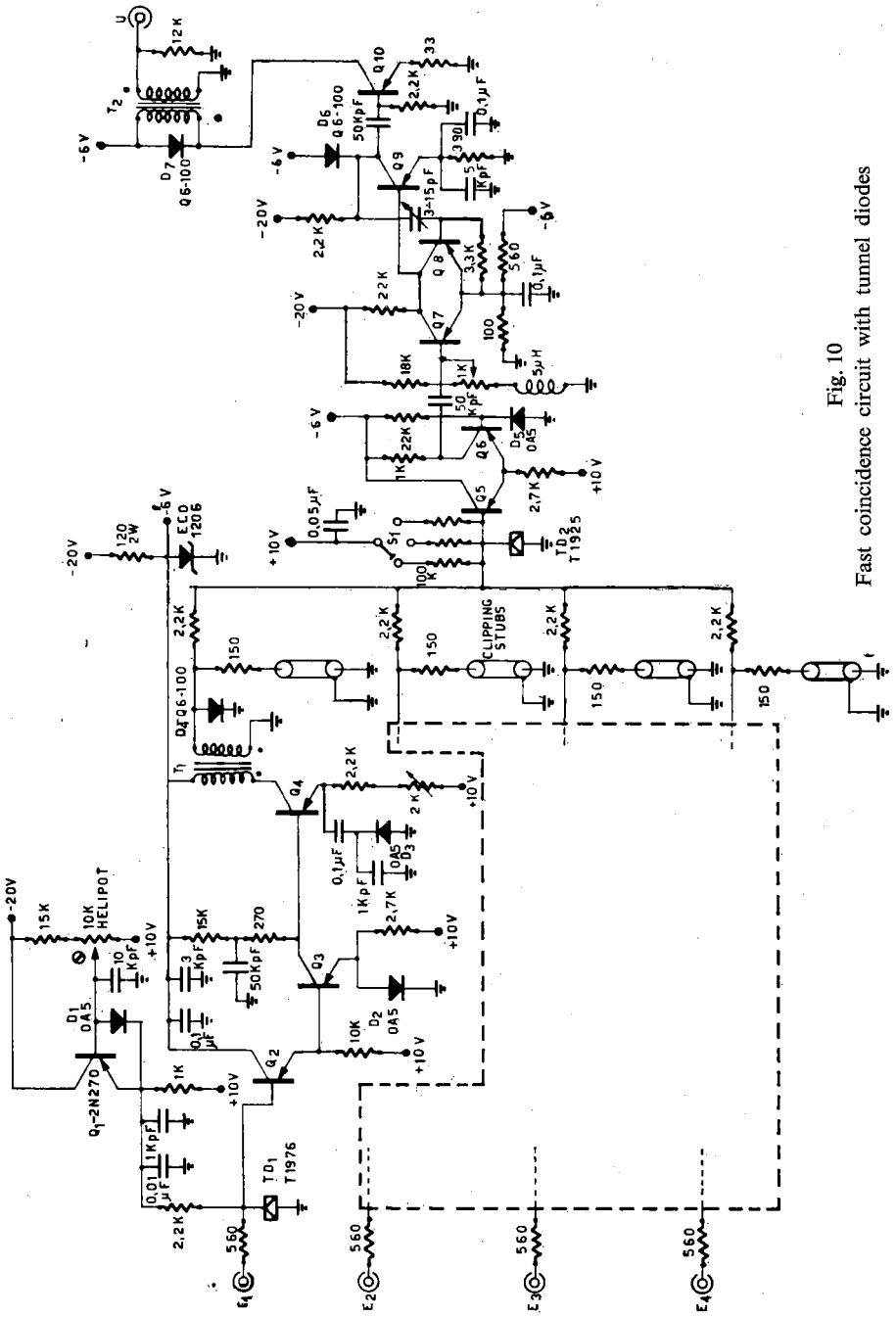

Fig. 10
Fast coincidence circuit with tunnel diodes

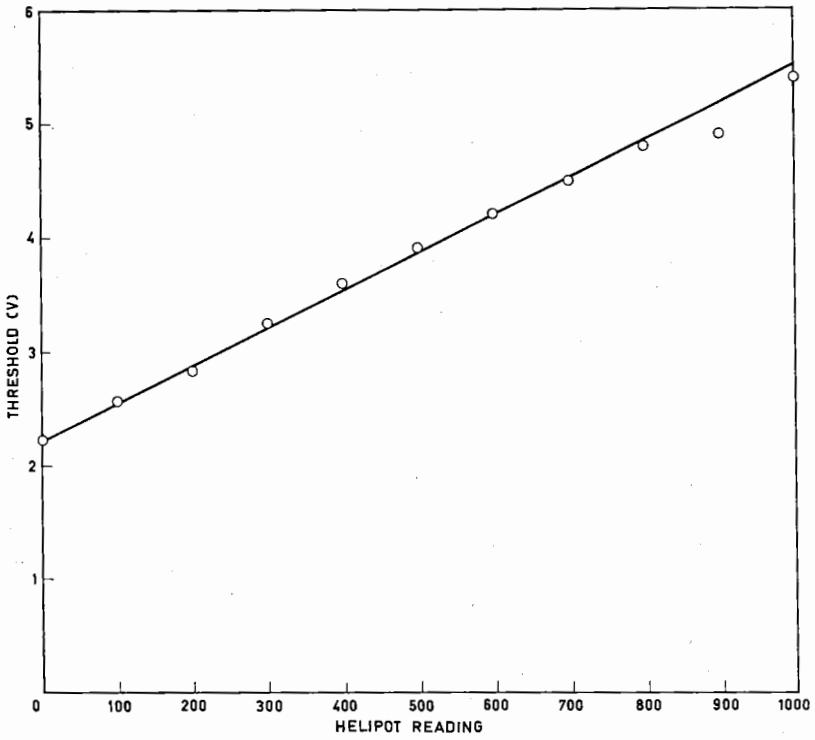

Fig. 11
Discriminator calibration curve

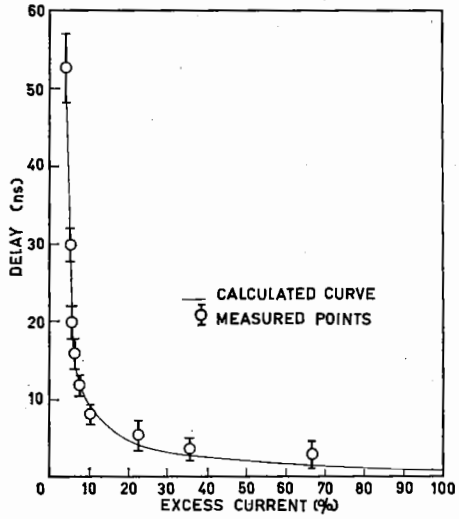

Fig. 12
Discriminator delay time

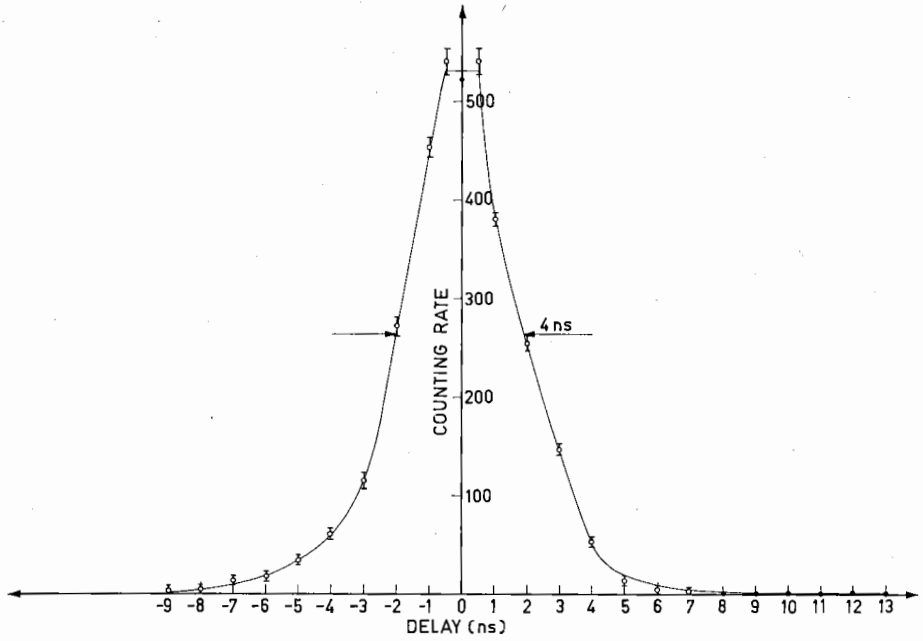

Fig. 13
Coincidence resolving time

ACKNOWLEDGEMENTS

The authors wish to express their thanks to professor I. F. Quercia for constant encouragement and advice and to Messrs. C. Dardini and R. Rizzi, who were of great help in setting up and testing the circuitry.

REFERENCES

[1] ESAKI, L., *Phys. Rev.* **109** (1958) 603.
[2] SOMMERS, H. S., *Proc. IRE* **47** (1959) 1201.
[3] CHASE, K. K. N., *Proc. IRE* **47** (1959) 1268.
[4] SPIEGEL, P., *Rev. Sci. Instr.* **31** (1960) 754.
[5] GOTO, E. *et al.*, *IRE Trans.* **EC-9** (1960) 25.
[6] RAJCHMANN, J., RCA Labs. (Private Communication.)
[7] CHOW, W. F., *IRE Trans.* **EC-9** (1960) 295.
[8] BERGMAN, R. H., *IRE Trans.* **EC-9** (1960) 430.
[9] Variations of Capacitance with voltage are neglected.
[10] MEY, J., *Rev. Sci. Instr.* **30** (1959) 282.
[11] DAVIDSOHN, U. S. *et al.*, *Electronic Design* (1960).
[12] BROWN, M., *Rev. Sci. Instr.* **30** (1959) 169.
[13] INFANTE, C., *Nucl. Instr. and Meth.* **9** (1960) 102.
[14] T 1975 made by Philco Corp.
[15] IN3130 made by Radio Corp. of America.
[16] MILLER, R. H., *Rev. Sci. Instr.* **30** (1959) 395.